Genome-wide RNAi screening identifies protein damage as a regulator of osmoprotective gene expression

Todd Lamitina*†, Chunyi George Huang‡, and Kevin Strange*§

*Departments of Anesthesiology and Pharmacology, Vanderbilt University, T4208 Medical Center North, 1161 21st Avenue South, Nashville, TN 37232; and ‡Department of Biological Chemistry, Johns Hopkins University School of Medicine, 725 North Wolfe Street, Baltimore, MD 21224

Edited by Martin Chalfie, Columbia University, New York, NY, and approved June 23, 2006 (received for review April 12, 2006)

The detection, stabilization, and repair of stress-induced damage are essential requirements for cellular life. All cells respond to osmotic stress-induced water loss with increased expression of genes that mediate accumulation of organic osmolytes, solutes that function as chemical chaperones and restore osmotic homeostasis. The signals and signaling mechanisms that regulate osmoprotective gene expression in animal cells are poorly understood. Here, we show that *gpdh-1* and *gpdh-2*, genes that mediate the accumulation of the organic osmolyte glycerol, are essential for survival of the nematode *Caenorhabditis elegans* during osmotic stress. Expression of GFP driven by the *gpdh-1* promoter ($P_{gpdh\text{-}1}$::*GFP*) is detected only during hypertonic stress but is not induced by other stressors. Using $P_{gpdh\text{-}1}$::*GFP* expression as a phenotype, we screened ≈16,000 genes by RNAi feeding and identified 122 that cause constitutive activation of *gpdh-1* expression and glycerol accumulation. Many of these genes function to regulate protein translation and cotranslational protein folding and to target and degrade denatured proteins, suggesting that the accumulation of misfolded proteins functions as a signal to activate osmoprotective gene expression and organic osmolyte accumulation in animal cells. Consistent with this hypothesis, 73% of these protein-homeostasis genes have been shown to slow age-dependent protein aggregation in *C. elegans*. Because diverse environmental stressors and numerous disease states result in protein misfolding, mechanisms must exist that discriminate between osmotically induced and other forms of stress-induced protein damage. Our findings provide a foundation for understanding how these damage-selectivity mechanisms function.

Caenorhabditis elegans | functional genomics | organic osmolytes | osmotic stress

The ability to detect, repair, and stabilize cellular and molecular damage induced by environmental stress is essential for cell survival and function. All organisms respond to environmental stress with increased expression of stress-protective genes. For example, heat shock causes protein denaturation and induces the expression of molecular chaperones that function to refold denatured proteins (1). Oxidative stress results in lipid and protein damage and activates the expression of antioxidant enzymes that detoxify free radicals (2).

Hypertonic stress causes cellular water loss, cell shrinkage, elevated cytoplasmic ionic strength, and increased expression of genes that mediate organic osmolyte accumulation. Organic osmolytes function as chemical chaperones and can be accumulated by cells to concentrations of hundreds of millimolar without adverse effects (3). Replacement of inorganic ions with organic osmolytes allows cells to maintain normal cytoplasmic ionic strength and survive in hypertonic environments (4, 5).

The effector mechanisms that mediate organic osmolyte accumulation are generally well defined. For example, in *Escherichia coli*, ProP is activated by hypertonicity and mediates uptake of compatible solutes such as proline, glycine betaine, and ectoine (6). Plants accumulate proline through hypertonicity-induced expression of biosynthetic enzymes (7). In yeast, hypertonicity induces expression of the glycerol biosynthesis enzyme glycerol 3-phosphate dehydrogenase (GPD), which mediates accumulation of the organic osmolyte glycerol (8). Cells of the renal inner medulla accumulate sorbitol and *myo*-inositol through increased expression of the sorbitol biosynthetic enzyme aldose reductase (9) and the sodium-coupled *myo*-inositol transporter SMIT (10).

The signals and signaling mechanisms that activate organic osmolyte accumulation in bacteria, plants, and yeast have been studied extensively (6, 7, 11). For example, genetic and molecular characterization of yeast has identified a MAP kinase signaling cascade that regulates hypertonicity-induced GPD expression (11). Activation of MAP kinase signaling is mediated by interaction of components of the cascade with the membrane protein Sho1. In animal cells, both the hypertonic stress signals and the signaling cascades that mediate osmosensitive gene expression are unknown. Sho1 homologs are absent from animal genomes, and, although animal homologs of yeast hypertonicity-activated kinases exist, none of them have been consistently shown to play a significant role in regulating osmosensitive gene expression (12, 13).

We have undertaken studies of the hypertonic stress response in *Caenorhabditis elegans* with the goal of exploiting this animal's genetic and molecular tractability to define animal cell osmosensing mechanisms. Recently, we demonstrated that *C. elegans* adapts to hypertonic stress by accumulating the organic osmolyte glycerol and that hypertonicity induces expression of glycerol biosynthetic enzymes (14). Here, we show that glycerol biosynthesis is essential for survival in hypertonic environments. Based on these findings, we developed an *in vivo* GFP reporter that reflects the activation state of signaling pathways controlling osmosensitive gene expression. Using genome-wide RNAi screening, we identified 122 gene inactivations that cause constitutive activation of this osmosensitive GFP reporter in the absence of hypertonic stress. The majority of these genes function normally to prevent the accumulation of damaged and denatured proteins in the cell cytoplasm. The results of our studies suggest the hypothesis that signaling pathways controlling osmosensitive gene expression in animal cells are activated, at least in part, by increased levels of hypertonicity-induced protein damage, specifically damage to proteins undergoing *de novo* synthesis.

Results and Discussion

When exposed to hypertonic stress, *C. elegans* accumulates the organic osmolyte glycerol by *de novo* synthesis (14). The worm

Conflict of interest statement: No conflicts declared.

This paper was submitted directly (Track II) to the PNAS office.

†Present address: Department of Physiology, University of Pennsylvania, 3700 Hamilton Walk, A306 Richards Building, Philadelphia, PA 19104.

§To whom correspondence should be addressed. E-mail: kevin.strange@vanderbilt.edu.

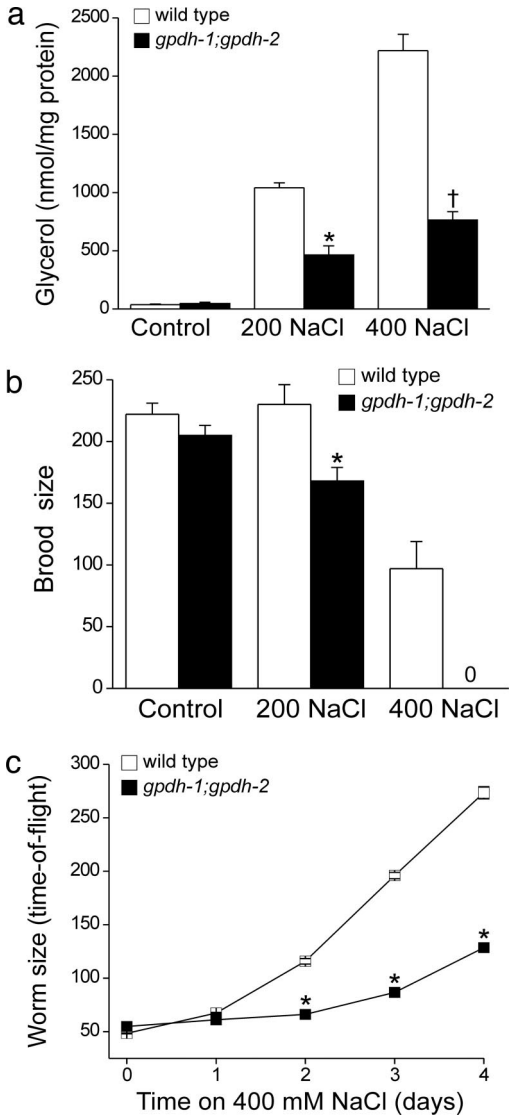

Fig. 1. *gpdh-1* and *gpdh-2* are required for adaptation to hypertonic stress. (*a*) Whole-animal glycerol levels in the wild type and *gpdh-1;gpdh-2* double mutants. L1 larvae were grown on control or 200 mM NaCl agar plates for 3–4 days before glycerol measurements. For measurements at 400 mM NaCl, L1 larvae were grown on 200 mM NaCl until the L4 stage of development and then shifted to 400 mM NaCl plates for 24 h. Values are means ± SE ($n = 3$). *, $P < 0.01$ compared with wild type; †, $P < 0.001$ compared with wild type. (*b*) Brood size in wild-type and *gpdh-1;gpdh-2* double-mutant worms. Values are means ± SE ($n = 9$–21). *, $P < 0.01$ compared with wild type. (*c*) Rate of growth in wild-type and *gpdh-1;gpdh-2* double-mutant worms exposed to 400 mM NaCl. Worm size was quantified as time-of-flight by using a COPAS Biosort. Values are means ± SE ($n > 300$). *, $P < 0.01$ compared with wild type.

genome contains two genes encoding glycerol-3-phosphate-dehydrogenase (*gpdh*), which catalyzes the rate-limiting step of glycerol biosynthesis. Microarray (data not shown) and Northern blot analyses (14) demonstrated that *gpdh-1* exhibits a strong and sustained transcriptional up-regulation during hypertonic stress, whereas *gpdh-2* is weakly and transiently up-regulated. To test the physiological role of glycerol biosynthesis in the hypertonic stress response, we used the deletion alleles of *gpdh-1* and *gpdh-2*, *ok1558*, and *kb33*, respectively. Although the rate of hypertonicity-induced glycerol accumulation was slowed in the *gpdh-1*-deletion mutant, steady-state glycerol levels under control and hypertonic conditions were similar to those in wild-type animals (data not shown). We therefore crossed *ok1558* and *kb33* worms to generate *gpdh-1;gpdh-2* double mutants. Glycerol levels (Fig. 1*a*), fertility (Fig. 1*b*), and growth rates (data not shown) of *gpdh-1(ok1558);gpdh-2(kb33)* worms were indistinguishable from wild-type animals under normal culture conditions. However, when exposed to hypertonic stress, *gpdh-1(ok1558);gpdh-2(kb33)* worms exhibited greatly reduced glycerol accumulation (Fig. 1*a*) and fertility (Fig. 1*b*) and grew considerably more slowly than wild-type animals (Fig. 1*c*). Therefore, GPDH-1- and GPDH-2-mediated glycerol accumulation is essential for survival in hypertonic environments.

GFP transcriptional reporters demonstrated constitutive expression of *gpdh-2* in the intestine, hypodermis, and excretory cell (Fig. 2*a*). In contrast, $P_{gpdh\text{-}1}$::*GFP* expression was virtually undetectable under control conditions but showed dramatic up-regulation in the intestine and hypodermis in worms exposed to hypertonicity (Fig. 2*a*). $P_{gpdh\text{-}1}$-*GFP* expression was proportional to the level of hypertonic stress (Fig. 2*b*), and the time course of expression (Fig. 2*c*) correlated well with that of glycerol accumulation (14). Heat shock (30°C; Fig. 2*c*), endoplasmic reticulum stress (10 μg/ml tunicamycin), cold (4°C), and oxidative stress (230 μM juglone and 100% O_2; data not shown) failed to activate $P_{gpdh\text{-}1}$::*GFP*. These data demonstrate that $P_{gpdh\text{-}1}$::*GFP* specifically reports activation of signaling pathways required for glycerol synthesis and adaptation of *C. elegans* to hypertonic stress.

To identify signals and signaling mechanisms that regulate osmoprotective gene expression in animal cells, we performed a genome-wide RNAi feeding screen based on $P_{gpdh\text{-}1}$::*GFP* expression. The $P_{gpdh\text{-}1}$::*GFP* reporter strain was used in this screen, because *gpdh-1* undergoes striking and sustained up-regulation in response to hypertonicity (ref. 14 and data not shown), and because $P_{gpdh\text{-}1}$::*GFP* expression was undetectable in the absence of hypertonic stress (Fig. 2*a*). L1-stage larvae on 20 mM NaCl growth plates were fed dsRNA-producing bacteria, and animals were visually scored for GFP expression after 3 days. We identified 106 gene inactivations that consistently activated $P_{gpdh\text{-}1}$::*GFP* expression in the absence of hypertonic stress (e.g., Fig. 3*a*). These genes are termed regulators of glycerol-3-phosphate-dehydrogenase expression (*rgpd*; Table 1; and see Table 2, which is published as supporting information on the PNAS web site).

Because our screen was based on activation of a GFP reporter, the genes we identified could encode regulators of transgene expression rather than components of signaling pathways controlling glycerol accumulation. To determine the role of *rgpd* genes in hypertonic stress resistance, we measured glycerol levels for a subset of *rgpd* genes in which viable and fertile loss-of-function mutants were available. Glycerol levels were significantly elevated 4- to 144-fold over control animals in worm strains harboring loss-of-function mutations in the genes tested (Fig. 3*b*).

Genome-wide RNAi screening results in significant numbers of false negatives (15). To identify additional *rgpd* genes, we queried the *C. elegans* Interactome, a genome-wide protein–protein interaction map comprising 3,228 genes and 5,685 yeast two-hybrid interactions (16). Forty-eight *rgpd* genes were present in the Interactome and showed few direct interactions. However, we identified 148 genes that interact with the *rgpd* genes (see Fig. 5, which is published as supporting information on the PNAS web site). RNAi constructs for 124 of these genes were present in our library. We rescreened these interacting genes (see *Methods*) and identified an additional 16 *rgpd* genes (see Fig. 5). The Interactome screen increased the *rgpd* genes by 15% to 122. This increase is consistent with false-negative rates of 10–30% that have been estimated for *C. elegans* genome-wide RNAi screens (15).

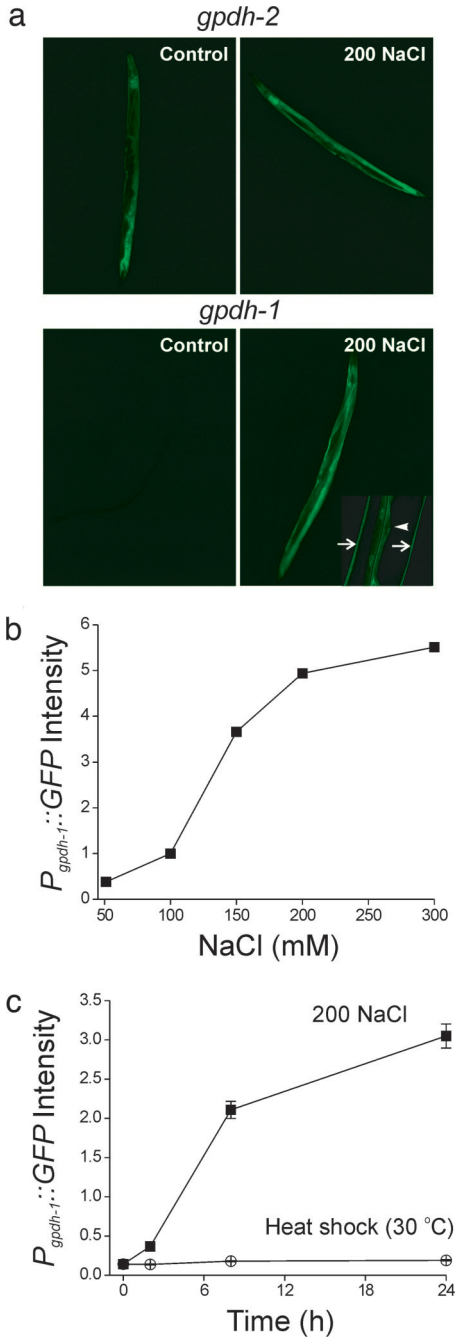

Fig. 2. *gpdh* transcriptional GFP reporters are activated by hypertonic stress. (*a Upper*) P_{gpdh-2}::*GFP* is constitutively expressed in the hypodermis, intestine, and excretory cell under control conditions. (*a Lower*) P_{gpdh-1}::*GFP* expression is undetectable under isotonic conditions and is dramatically elevated after exposure to 200 mM NaCl. P_{gpdh-1}::*GFP* is expressed in the intestine (*Lower Right*, arrowhead) and hypodermis (*Lower Right*, arrows). (*b*) Effect of NaCl concentration on P_{gpdh-1}::*GFP* expression in young adult worms. Animals were placed on agar plates containing the indicated amounts of NaCl for 24 h. Values are means ± SE ($n >$ 1,000). P_{gpdh-1}::*GFP* expression was also induced by hypertonic KCl, sucrose, or sorbitol (data not shown), indicating that *gpdh-1* expression is regulated specifically by hypertonicity-induced water loss rather than elevated Na^+ or Cl^- levels. (*c*) Changes in P_{gpdh-1}::*GFP* expression in young adult worms during hypertonic stress or heat shock (30°C). Values are means ± SE ($n > 150$). GFP expression in *b* and *c* was quantified by using a COPAS BioSort and normalized to time-of-flight (i.e., GFP fluorescence divided by time-of-flight).

Many of the *rgpd* genes encode conserved proteins, and 72 of them have human homologs (Table 2). Expression patterns have been determined by using GFP reporters for 35 of the genes, and

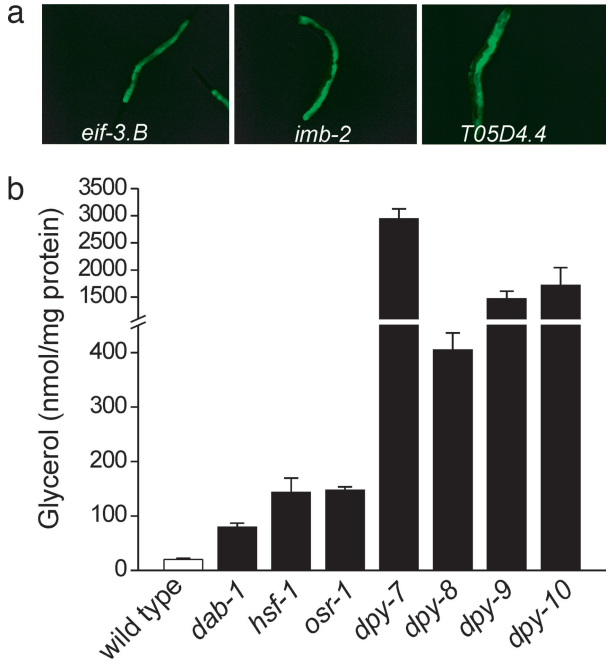

Fig. 3. Loss of gene function by RNAi or mutation causes constitutive expression of P_{gpdh-1}::*GFP* and glycerol accumulation in the absence of hypertonic stress. (*a*) Examples of genes identified in genome-wide RNAi screening that activate P_{gpdh-1}::*GFP* expression when silenced. (*b*) Glycerol content in worms harboring loss-of-function mutations in genes identified by RNAi screening. Values are means ± SE ($n = 3$). All glycerol levels in mutant worms were significantly ($P < 0.02$) different from wild type.

30 are coexpressed with *gpdh-1* in the hypodermis and/or intestine (Table 2) (17). *rgpd* gene functions fell into six defined cellular processes and a group of genes with unassigned functions (Tables 1 and 2). The defined processes include protein homeostasis, extracellular matrix, signaling, metabolism, protein trafficking, and transcriptional regulation.

Four of the extracellular matrix genes encode the collagens DPY-7, DPY-8, DPY-9, and DPY-10. Loss-of-function mutations in these genes increased P_{gpdh-1}::*GFP* expression (data not shown) and glycerol accumulation (Fig. 3*b*). The DPY collagens are secreted proteins that likely function extracellularly. Interestingly, we also identified 10 genes with unassigned functions that are predicted to encode secreted proteins (Tables 1 and 2). Secreted proteins have been shown to play important roles in mechanotransduction. For example, MEC-1 and MEC-9 are secreted by *C. elegans* touch neurons and genetically interact with the collagen MEC-5 (18, 19). These three proteins are essential components of the *C. elegans* touch neuron mechanosensory complex (20). Similarly, DPY collagens and other secreted proteins could function to detect hypertonic stress-induced mechanical signals. In vertebrates, collagens and integrins function in cellular mechanotransduction (21, 22) and osmotic stress-induced signaling processes (23–26).

dpy-7 and *dpy-10* have been shown to suppress temperature-sensitive mutations in several unrelated genes (27, 28). Phenotypes associated with temperature-sensitive mutations are thought to be due to misfolding of the mutated protein that is reduced at low temperatures (29, 30). Because organic osmolytes such as glycerol aid in the refolding of denatured proteins (31), the ability of the *dpy* mutants to suppress temperature-sensitive gene mutations might be a general property of all *rgpd* genes that activate *gpdh-1* expression and cause glycerol accumulation (Fig. 3*b*).

Surprisingly, the majority (44%, or 54 of 122) of *rgpd* genes fell into a category defined as protein homeostasis (Table 1). These

Table 1. Summary of gene knockdowns that cause constitutive *gpdh-1* expression

Process (no. of genes)	Molecular function (no. of genes)	Gene example	Description	Human homolog
Protein homeostasis (54)				
Protein synthesis (38)	Translation initiation (10)	B0511.10/*eif-3.E*	Translation initiation factor 3, subunit e	EIF3S6
	tRNA synthetase (10)	F22D6.3/*nrs-1*	Asparaginyl-tRNA synthetase	NARS
	RNA processing (18)	W08E3.1/*snr-2*	U1 snRNP component	SNRPN
Protein folding (7)	Chaperonins (4)	K01C8.10/*cct-4*	Chaperonin complex, δ-subunit	CCT4
	Hsp70 (1)	F26D10.3/*hsp-1*	Molecular chaperones HSP70 superfamily	HSPA8
Protein degradation (9)	26S proteasome (4)	C23G10.4/*rpn-2*	26S proteasome-regulatory complex	PSMD1
Extracellular matrix (5)	Collagen (4)	T14B4.7/*dpy-10*	Collagens (types IV and XIII)	Collagen α IV
Signaling (15)	Scaffolding (2)	ZK849.2	PDZ domain	GOPC
	Transduction (6)	F38H4.9/*let-92*	Ser/thr protein phosphatase 2A, catalytic subunit	PPP2CB
Metabolism (9)	Trehalose synthesis (1)	H13N06.3/*gob-1*	Trehalose 6-phosphate synthase	None
Protein trafficking (6)	Nuclear import (1)	R06A4.4/*imb-2*	Nuclear transport receptor	TNPO2
Transcriptional regulation (9)	CCR4/NOT complex (2)	F57B9.2/*ntl-1*	Negative regulator of transcription	CNOT1
Unassigned function (24)	Secreted protein (10)	C32E12.3/*osr-1*	Osmotic stress-resistance protein	None
	Unknown function (14)	B0035.11	Uncharacterized conserved protein	LEO1

genes encode proteins required for RNA processing, protein synthesis, protein folding, and protein degradation. Protein homeostasis genes function to maintain levels of properly folded and functioning cellular proteins. Inhibition of protein homeostasis genes is expected to increase the levels of damaged cellular proteins. Recent studies by Nollen *et al.* (32) support this idea. Wild-type GFP expressed in *C. elegans* muscle cells is distributed uniformly in the cytoplasm. However, modified GFPs containing repeats of glutamine undergo age-dependent aggregation (33). Genome-wide RNAi screening identified 187 genes that function to slow aging-induced protein aggregation (32). We found that 34 of the 122 *rgpd* genes overlapped with this 187-gene data set (Table 2), a 24-fold greater overlap than expected by chance alone ($P < 0.001$). Strikingly, 25 of the 34 overlapping genes are predicted to function in RNA processing, protein synthesis, protein folding, and protein degradation. Thus, genes that function to prevent protein aggregation also function to inhibit *gpdh-1* expression. When the function of these genes is disrupted, damaged and denatured proteins accumulate in cells, and *gpdh-1* expression is increased, leading to glycerol accumulation. Our results are consistent with a model in which increased levels of damaged or denatured proteins act as a signal that triggers osmoprotective gene expression and organic osmolyte accumulation (Fig. 4). Accumulation of organic osmolytes is expected to stabilize protein structure and decrease protein misfolding (31), which, in turn, would serve to autoregulate pathway activity.

Interestingly, protein damage induced by numerous stressors including heat shock (Fig. 2*c*) does not activate $P_{gpdh\text{-}1}$::*GFP*. Thus, osmotic stress must cause a type of protein damage that selectively activates *gpdh-1* expression. Recent studies in eukaryotic cells suggest a mechanism for how osmotic stress-induced damage may be discriminated from other forms of protein damage. Albanese *et al.* (34) demonstrated that eukaryotes have at least two distinct systems for detecting and repairing protein misfolding. Canonical heat-shock proteins (HSPs) function to refold stress-denatured proteins (35). In contrast, chaperones that are linked to protein synthesis (CLIPS) function to regulate *de novo* protein folding (34).

The results of our screen suggest that *de novo* protein folding associated with protein synthesis plays a critical role in the hypertonic stress response. Canonical HSPs were not detected in our screen. Instead, the four T complex chaperones and *hsp-1*/F26D10.3 are predicted CLIPS (Tables 1 and 2). Furthermore, RNAi silencing of 38 genes involved in RNA processing and protein translation activates $P_{gpdh\text{-}1}$::*GFP* expression (Tables 1 and 2). In both cases, inhibition of these genes is predicted to disrupt protein synthesis.

Previous studies have shown that hypertonic stress, but not heat or oxidative stress, inhibits protein synthesis in yeast. Inhibition is transient, and recovery occurs via a Hog1p-dependent process that likely requires glycerol accumulation (36). Importantly, the initiation and elongation steps of protein synthesis are inhibited *in vitro* by increases in salt concentration of as little as 10 mM, and salt-induced inhibition is fully reversed by organic osmolytes (37). Inhibition of elongation causes disengagement of actively translating ribosomes from mRNAs and premature termination of protein translation, resulting in accumulation of incomplete and aberrantly folded polypeptides. Because cell shrinkage increases cytoplasmic salt concentration, these observations are consistent with a model in which *gpdh-1* expression is specifically activated by osmotically induced disruption of new protein synthesis and cotranslational folding

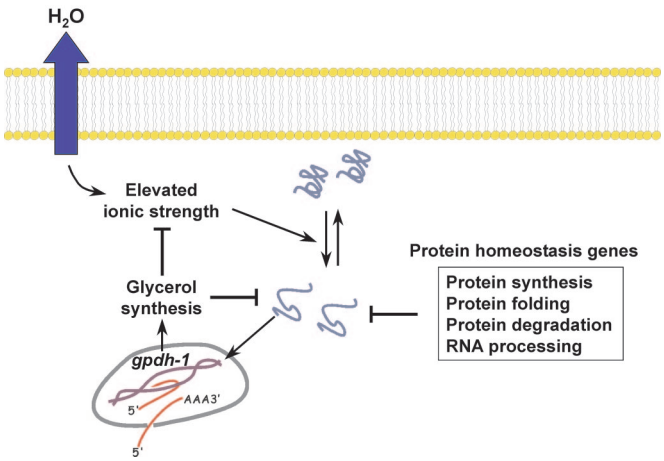

Fig. 4. Model for regulation of osmosensitive gene expression by disruption of protein homeostasis. Hypertonic stress-induced water loss causes elevated cytoplasmic ionic strength, which, in turn, causes protein damage. Damaged proteins function as a signal that activates *gpdh-1* expression and glycerol synthesis. Glycerol replaces inorganic ions in the cytoplasm and functions as a chemical chaperone that aids in the refolding of misfolded proteins. Loss of function of protein homeostasis genes also causes accumulation of damaged proteins and activation of *gpdh-1* expression.

rather than by denaturation of existing proteins. Such a mechanism would allow cells to discriminate between osmotically induced protein damage and other forms of stress-induced damage. Our proposed model is analogous to the unfolded protein response, which is an intracellular signaling and transcriptional/translational program activated by the accumulation of unfolded proteins in the endoplasmic reitculum (ER) lumen that functions to restore ER protein homeostasis (38).

The response of a multicellular organism such as *C. elegans* to hypertonic stress likely involves the integration of a number of hypertonicity-induced signals and signal-transduction pathways. However, our RNAi studies indicate that disruption of protein homeostasis alone is sufficient to activate cellular osmoprotective pathways. Given that a wide range of environmental stressors induces protein damage, mechanisms must exist that discriminate between osmotically induced protein damage and other forms of stress-induced protein damage. Our findings provide a new foundation for understanding how these damage-selectivity mechanisms function and for defining the signaling pathways by which animal cells respond to osmotic stress. Because accumulation of misfolded proteins is a hallmark of diseases such as Alzheimer's and Parkinson's (39), understanding the molecular events underlying the detection of osmotically induced protein damage will provide an important paradigm for defining the cellular response to disease-induced protein damage.

Methods

***C. elegans* Strains.** All strains used in this study were derived from the N2 Bristol wild-type strain. Unless otherwise noted, worms were cultured at 20°C. The following strains were used: LGI-RB1032 [*osr-1(ok959)*], PS3551 [*hsf-1(sy441)*], LGII-VC616 [*dab-1(gk216)*], CB128 [*dpy-10(e128)*], LGIV-CB12 [*dpy-9(e12)*], LGX-CB88 [*dpy-7(e88)*], and CB130 [*dpy-8(e130)*].

gpdh-1(ok1558) was obtained from the *Caenorhabditis* Genetics Center (University of Minnesota, Minneapolis). We generated *gpdh-2(kb33)* by PCR-based screening. Both mutants were outcrossed to wild-type animals three times and exhibited no gross phenotypic defects as homozygotes. *ok1558* encodes a 1,227-bp deletion in F47G4.3 (flanking sequences, tgcaactgat/ctagaaacca), and *kb33* encodes a 758-bp deletion in K11H3.1 (flanking sequences, tttattcctc/aagaactgtt). *gpdh-1(ok1558) I;gpdh-2(kb33)III* animals were generated by crossing and PCR genotyping.

Plasmid Construction. To create $P_{gpdh\text{-}1}$::*GFP*, a 3.3-kb PCR fragment, containing 3 kb of sequence 5′ to the start ATG and the first six amino acids from exon 2, was cloned into BamHI and SphI sites of pPD95.75. To create $P_{gpdh\text{-}2}$::*GFP*, a 4.4-kb PCR fragment, containing 2.3 kb of sequence 5′ to the start ATG and the first eight amino acids of exon 2 of the K11H3.1a gene, was cloned into SphI sites of pPD95.75. Both constructs were confirmed by sequencing. Primer sequences are available upon request.

Transgenics. Wild-type animals were injected with 75 ng/μl *rol-6* marker pRF4 and 25 ng/μl GFP construct by using standard methods (40). Three of the $P_{gpdh\text{-}1}$::*GFP* and two of the $P_{gpdh\text{-}2}$::*GFP* lines generated showed identical patterns of GFP expression under control and hypertonic growth conditions. Array *kbEx144* was used to generate the integrated strain *kbIs5*. Integration was carried out by exposing ≈50 *kbEx144* L4 animals to 30,000 μJ/cm^2 generated from a UV cross-linker (Hoeffer Instruments, San Francisco, CA). A single integrated line segregating 100% *rol-6* animals was isolated and outcrossed three times to wild-type animals to generate *kbIs5* [$P_{gpdh\text{-}1}$::*GFP;rol-6(su1006)*], which was used in all subsequent studies.

Genome-Wide RNAi Screening. Genome-wide RNAi screening was carried out by using a commercially available RNAi feeding library (MRC Geneservice, Cambridge, U.K.). Single colonies were inoculated into 100 μl of LB media containing 25 μg/ml carbenicillin and grown for 6–8 h at 37°C. Twenty microliters of each culture was spotted onto individual wells of 24-well nematode growth medium (NGM) agar plates containing 20 mM NaCl, 1 mM isopropyl β-D-thiogalactoside (IPTG), and 25 μg/ml carbenicillin. After overnight induction of dsRNA, 30–40 L1-stage animals were dispensed into each well. GFP expression was monitored after 72 h at 16°C by using an M2Bio fluorescence microscope (Zeiss, Thornwood, NY). Clones were scored as positive if at least five animals exhibited visible GFP fluorescence. These clones were rescreened in quadruplicate, and those that induced GFP expression in at least three of four trials were considered bona fide regulators of gpdh-1 expression, or *rgpd* genes.

rgpd genes present in the *C. elegans* Interactome (16), and their interacting proteins were rescreened for the *rgpd* phenotype by RNAi. Bacterial strains were grown as described above. Forty microliters of each bacterial culture was spotted onto individual wells of 24-well NGM RNAi plates and left at room temperature overnight. Five to 10 L1-stage animals were dispensed into each well and allowed to develop into gravid adults at 16°C. After laying >20 eggs, the adults were removed from the plate. F1 RNAi-treated animals were examined for GFP expression 3–4 days after hatching. The screen was repeated twice, and positive clones were assigned a score based on the level of GFP induction from 1 (weak) to 3 (strong). Scores from each screen were summed, and clones that had a total score of >2 were considered to confer an *rgpd* phenotype. Both the genome-wide and Interactome screens were performed blind to the identity of the genes being screened.

Measurement of Brood Size and Rate of Growth. L1-stage worms were placed on NGM plates containing 51, 200, or 400 mM NaCl. After 2–4 days, single L4-stage hermaphrodites were placed into individual wells of 24-well plates. Worms were transferred to new wells every day until egg-laying ceased (3–4 days). Brood size was determined by summing the number of viable progeny in each well.

Growth rate was estimated by transferring L1-stage worms onto NGM plates containing 400 mM NaCl. Worms were washed off plates with M9 solution containing 400 mM NaCl at 24 h intervals, and animal size was quantified as time-of-flight, which was measured using a COPAS Biosort (Union Biometrica, Somerville, MA). Time-of-flight is a direct measure of worm axial length (41).

Glycerol Measurements. Hypochlorite-synchronized L1-stage larvae were placed onto enriched peptone plates streaked with NA22 bacteria. After 3–4 days at 20°C, gravid worms were washed off plates and processed for glycerol measurements as described (14).

Statistical Analyses. Data are presented as means ± SE. Statistical significance was determined by using Student's two-tailed *t* test for unpaired means. Significance of the overlap between two sets of genes was determined by calculating the representation factor, which is the total number of overlapping genes divided by the expected number of overlapping genes. Calculation of the representation factor and *P* value were carried out as described (42). *P* values of <0.05 were considered to indicate significance.

This work was supported by National Institutes of Health (NIH) Grants DK61168 and DK64743 (to K.S.) T.L. was supported by a fellowship from the National Kidney Foundation. Some nematode strains used in this work were provided by the *Caenorhabditis* Genetics Center, which is funded by the NIH National Center for Research Resources.

1. Young, J. C., Agashe, V. R., Siegers, K. & Hartl, F. U. (2004) *Nat. Rev. Mol. Cell Biol.* **5,** 781–791.
2. Liu, H., Colavitti, R., Rovira, I. I. & Finkel, T. (2005) *Circ. Res.* **97,** 967–974.
3. Yancey, P. H. (2005) *J. Exp. Biol.* **208,** 2819–2830.
4. Burg, M. B. (1995) *Am. J. Physiol.* **268,** F983–F996.
5. Yancey, P. H., Clark, M. E., Hand, S. C., Bowlus, R. D. & Somero, G. N. (1982) *Science* **217,** 1214–1222.
6. Wood, J. M., Bremer, E., Csonka, L. N., Kraemer, R., Poolman, B., van der Heide, T. & Smith, L. T. (2001) *Comp. Biochem. Physiol. A* **130,** 437–460.
7. Hasegawa, P. M., Bressan, R. A., Zhu, J. K. & Bohnert, H. J. (2000) *Annu. Rev. Plant Physiol. Plant Mol. Biol.* **51,** 463–499.
8. Hohmann, S. (2002) *Microbiol. Mol. Biol. Rev.* **66,** 300–372.
9. Smardo, F. L., Jr., Burg, M. B. & Garcia-Perez, A. (1992) *Am. J. Physiol.* **262,** C776–C782.
10. Yamauchi, A., Nakanishi, T., Takamitsu, Y., Sugita, M., Imai, E., Noguchi, T., Fujiwara, Y., Kamada, T. & Ueda, N. (1994) *J. Am. Soc. Nephrol.* **5,** 62–67.
11. O'Rourke, S. M., Herskowitz, I. & O'Shea, E. K. (2002) *Trends Genet.* **18,** 405–412.
12. Kwon, H. M., Itoh, T., Rim, J. S. & Handler, J. S. (1995) *Biochem. Biophys. Res. Commun.* **213,** 975–979.
13. Kultz, D., Garcia-Perez, A., Ferraris, J. D. & Burg, M. B. (1997) *J. Biol. Chem.* **272,** 13165–13170.
14. Lamitina, S. T., Morrison, R., Moeckel, G. W. & Strange, K. (2004) *Am. J. Physiol.* **286,** C785–C791.
15. Simmer, F., Moorman, C., Van Der Linden, A. M., Kuijk, E., Van Den Berghe, P. V., Kamath, R., Fraser, A. G., Ahringer, J. & Plasterk, R. H. (2003) *PLoS Biol.* **1,** E12.
16. Li, S., Armstrong, C. M., Bertin, N., Ge, H., Milstein, S., Boxem, M., Vidalain, P. O., Han, J. D., Chesneau, A., Hao, T. *et al.* (2004) *Science* **303,** 540–543.
17. McKay, S. J., Johnsen, R., Khattra, J., Asano, J., Baillie, D. L., Chan, S., Dube, N., Fang, L., Goszczynski, B., Ha, E. *et al.* (2003) *Cold Spring Harbor Symp. Quant. Biol.* **68,** 159–169.
18. Gu, G., Caldwell, G. A. & Chalfie, M. (1996) *Proc. Natl. Acad. Sci. USA* **93,** 6577–6582.
19. Du, H., Gu, G., William, C. M. & Chalfie, M. (1996) *Neuron* **16,** 183–194.
20. Emtage, L., Gu, G., Hartwieg, E. & Chalfie, M. (2004) *Neuron* **44,** 795–807.
21. DeMali, K. A., Wennerberg, K. & Burridge, K. (2003) *Curr. Opin. Cell Biol.* **15,** 572–582.
22. ffrench-Constant, C. & Colognato, H. (2004) *Trends Cell Biol.* **14,** 678–686.
23. Vom, D. S., Schliess, F., Reissmann, R., Gorg, B., Weiergraber, O., Kocalkova, M., Dombrowski, F. & Haussinger, D. (2003) *J. Biol. Chem.* **278,** 27088–27095.
24. Sheikh-Hamad, D., Youker, K., Truong, L. D., Nielsen, S. & Entman, M. L. (2000) *Am. J. Physiol.* **279,** C136–C146.
25. Browe, D. M. & Baumgarten, C. M. (2003) *J. Gen. Physiol.* **122,** 689–702.
26. Moeckel, G. W., Zhang, L., Chen, X., Rossini, M., Zent, R. & Pozzi, A. (2006) *Am. J. Physiol.* **290,** F223–F231.
27. Nishiwaki, K. & Miwa, J. (1998) *Mol. Gen. Genet.* **259,** 2–12.
28. Levy, A. D., Yang, J. & Kramer, J. M. (1993) *Mol. Biol. Cell* **4,** 803–817.
29. Gidalevitz, T., Ben Zvi, A., Ho, K. H., Brignull, H. R. & Morimoto, R. I. (2006) *Science* **311,** 1385–1386.
30. Van Dyk, T. K., Gatenby, A. A. & LaRossa, R. A. (1989) *Nature* **342,** 451–453.
31. Auton, M. & Bolen, D. W. (2005) *Proc. Natl. Acad. Sci. USA* **102,** 15065–15068.
32. Nollen, E. A., Garcia, S. M., van Haaften, G., Kim, S., Chavez, A., Morimoto, R. I. & Plasterk, R. H. (2004) *Proc. Natl. Acad. Sci. USA* **101,** 6403–6408.
33. Morley, J. F., Brignull, H. R., Weyers, J. J. & Morimoto, R. I. (2002) *Proc. Natl. Acad. Sci. USA* **99,** 10417–10422.
34. Albanese, V., Yam, A. Y., Baughman, J., Parnot, C. & Frydman, J. (2006) *Cell* **124,** 75–88.
35. Gasch, A. P., Spellman, P. T., Kao, C. M., Carmel-Harel, O., Eisen, M. B., Storz, G., Botstein, D. & Brown, P. O. (2000) *Mol. Biol. Cell* **11,** 4241–4257.
36. Uesono, Y. & Toh, E. (2002) *J. Biol. Chem.* **277,** 13848–13855.
37. Brigotti, M., Petronini, P. G., Carnicelli, D., Alfieri, R. R., Bonelli, M. A., Borghetti, A. F. & Wheeler, K. P. (2003) *Biochem. J.* **369,** 369–374.
38. Schroder, M. & Kaufman, R. J. (2005) *Annu. Rev. Biochem.* **74,** 739–789.
39. Selkoe, D. J. (2004) *Nat. Cell Biol.* **6,** 1054–1061.
40. Mello, C. C. & Fire, A. (1995) in *Caenorhabditis elegans; Modern Biological Analysis of an Organism*, eds. Epstein, H. F. & Shakes, D. C. (Academic, San Diego), pp. 452–482.
41. Pulak, R. (2006) in *C. elegans: Methods and Applications* (Humana Press, Inc., Totowa, NJ), in press.
42. Kim, S. K., Lund, J., Kiraly, M., Duke, K., Jiang, M., Stuart, J. M., Eizinger, A., Wylie, B. N. & Davidson, G. S. (2001) *Science* **293,** 2087–2092.

Table 2. Description of regulators of gpdh-1 expression (*rgpd*) genes

			Homologs[§]			
Sequence/gene name*	Causes protein aggregation[†]	Description (expression pattern)[‡]	*Hs*	*Dm*	*Cb*	*Sc*
Protein homeostasis						
K04G2.1	Y	Translation initiation factor 2, beta subunit				
B0511.10/*eif-3.E*	Y	Translation initiation factor 3, subunit e (I, H, O)				
Y39G10AR.8	Y	Translation initiation factor 2, gamma subunit (I, O)				
F22B5.2/*eif-3.G*		Translation initiation factor 3, subunit g				
D2085.3		Translation initiation factor 2B, epsilon subunit (I, H, O)				
D2013.7/*eif-3.F*		Translation initiation factor 3, subunit f				
Y54E2A.11/*eif-3.B*		Translation initiation factor 3, subunit b (O)				
F57B9.3	Y	Translation initiation factor 4F, helicase subunit				
C27D11.1/*egl-45*	Y	Translation initiation factor 3, subunit a				
C37C3.2	Y	Translation initiation factor 5				
F22D6.3/*nrs-1*		Asparaginyl-tRNA synthetase				

			Homologs[§]			
Sequence/gene name*	Causes protein aggregation[†]	Description (expression pattern)[‡]	*Hs*	*Dm*	*Cb*	*Sc*
T08B2.9/*frs-1*		Phenylalanyl-tRNA synthetase, beta subunit				
T02G5.9/*krs-1*		Lysyl-tRNA synthetase (I, H, O)				
F22B5.9/*frs-2*	Y	Phenylalanyl-tRNA synthetase				
R74.1/*lrs-1*		Leucyl-tRNA synthetase				
F26F4.10/*rrt-1*		Arginyl-tRNA synthetase				
T10F2.1/*grs-1*		Glycyl-tRNA synthetase				
C47E12.1/*srs-2*		Seryl-tRNA synthetase				
R11A8.6/*irs-1*		Isoleucyl-tRNA synthetase (H, O)				
Y80D3A.1/*wrs-1*		Tryptophanyl-tRNA synthetase				
C32E8.11		N-end rule pathway, recognition component UBR1				
C36B1.4/*pas-4*	Y	20S proteasome, regulatory subunit alpha type (O)				
Y46G5A.6[¶]	Y	RNA helicase BRR2, DEAD-box superfamily				

			Homologs[§]			
Sequence/gene name*	Causes protein aggregation[†]	Description (expression pattern)[‡]	*Hs*	*Dm*	*Cb*	*Sc*
ZK20.5/*rpn-12*		26S proteasome regulatory complex, subunit RPN12/PSMD8				
C23G10.4/*rpn-2*		26S proteasome regulatory complex (I, H, O)				
F57B9.10/*rpn-6*	Y	26S proteasome regulatory complex				
T22D1.9/*rpn-1*		26S proteasome regulatory complex				
C35B1.1/*ubc-1*		Ubiquitin-protein ligase (I, H, O)				
CD4.6/*pas-6*	Y	20S proteasome, regulatory subunit alpha type				
Y53C10A.12/*hsf-1*	Y	Heat shock transcription factor				
W08F4.8/*cdc-37*		Cell division cycle 37 protein, CDC37				
K01C8.10/*cct-4*	Y	Chaperonin complex component, TCP-1 δ-subunit (I, O)				
T21B10.7/*cct-2*	Y	Chaperonin complex component, TCP-1 β-subunit (H,O)				
F26D10.3/*hsp-1*	Y	Molecular chaperones HSP70/HSC70, HSP70 superfamily (I,O)				
Y55F3AR.3/*cct-8*		Chaperonin complex component, TCP-1 θ-subunit				

			Homologs[§]			
Sequence/gene name*	Causes protein aggregation[†]	Description (expression pattern)[‡]	*Hs*	*Dm*	*Cb*	*Sc*
T10B5.5/*cct-7*	Y	Chaperonin complex component, TCP-1 η-subunit (O)				
T21G5.5/*star-2*		RNA-binding protein Sam68 and related KH domain proteins				
F37E3.1		Nuclear cap-binding complex, subunit NCBP1/CBP80				
Y110A7A.8	Y	mRNA splicing factor PRP31				
K02F2.3/*tag-203*	Y	Splicing factor 3b, subunit 3				
W08E3.1/*snr-2*	Y	U1 snRNP component				
Y71F9B.4/*snr-7*	Y	Small nuclear ribonucleoprotein G				
F26A3.2		Nuclear cap-binding protein complex, subunit CBP20, RRM superfamily				
W07E6.4/*prp-21*		Splicing factor 3a, subunit 1				
T13H5.4	Y	Splicing factor 3a, subunit 3				
T28D9.10/*snr-3*	Y	Small nuclear ribonucleoprotein SMD1 and related snRNPs				
C18D11.4/*rsp-8*		RRM domain; splicing factor (I, O)				

			Homologs[§]			
Sequence/gene name*	Causes protein aggregation[†]	Description (expression pattern)[‡]	*Hs*	*Dm*	*Cb*	*Sc*
T08A11.2	Y	Splicing factor 3b, subunit 1				
ZK652.1/*snr-5*	Y	Small nuclear ribonucleoprotein (snRNP) SMF (I, H, O)				
W08D2.7		Nuclear exosomal RNA helicase MTR4, DEAD-box superfamily (I, O)				
F19F10.9		U4/U6.U5 snRNP associated protein				
Y59A8B.6		HAT repeat protein				
K07C5.6		RNA splicing factor Slu7p				
Y116A8C.42/*snr-1*	Y	Small nuclear ribonucleoprotein Sm D3 (H, O)				
Extracellular matrix						
T14B4.7/*dpy-10*[¶]		Collagens (type IV and type XIII) and related proteins				
T21D12.2/*dpy-9*[¶]		Collagens (type IV and type XIII) and related proteins				
C31H2.2/*dpy-8*[¶]		Collagens (type IV and type XIII) and related proteins				
F46C8.6/*dpy-7*[¶]		Collagens (type IV and type XIII) and related proteins (H)				

			Homologs[§]			
Sequence/gene name*	Causes protein aggregation[†]	Description (expression pattern)[‡]	*Hs*	*Dm*	*Cb*	*Sc*
M60.2[¶]		Placental protein 11				
Signalling						
ZK849.2		PDZ domain				
T08G11.4		Methylase				
R06A10.2/*gsa-1*		G protein subunit Galphas, small G protein superfamily (I, O)				
F26H9.6/*rab-5*	Y	GTPase Rab5/YPT51 and related small G protein superfamily GTPases				
EGAP2.3/*pho-1*[¶]		Lysosomal and prostatic acid phosphatases (I)				
M110.5/*dab-1*	Y	Adaptor protein disabled (I, H, O)				
Y110A2AL.8/*ptc-3*	Y	Membrane protein patched/PTCH				
C54A12.1/*ptr-6*		Predicted membrane protein, patched superfamily				
B0285.1		Cdc2-related protein kinase (I, H, O)				
F20H11.2/*nsh-1*		Nuclear helicase MOP-3/SNO, DEAD-box superfamily				

			Homologs[§]			
Sequence/gene name*	Causes protein aggregation[†]	Description (expression pattern)[‡]	*Hs*	*Dm*	*Cb*	*Sc*
Y11D7A.9		FGF activating protein 1				
F33D4.2/*itr-1*		Inositol 1,4,5-trisphosphate receptor (I, O)				
C07G1.5/*hgrs-1*		Membrane trafficking and cell signaling protein HRS, contains VHS and FYVE domains				
F38H4.9/*let-92*		Serine/threonine protein phosphatase 2A, catalytic subunit (I, O)				
F58E2.9/*srz-23*[¶]		7-transmembrane receptor				
Metabolism						
T10E9.9		Short-chain acyl-CoA dehydrogenase				
F32H2.5		Animal-type fatty acid synthase and related proteins				
Y105E8B.5		Hypoxanthine-guanine phosphoribosyltransferase				
F42A8.2/*tag-55*		Succinate dehydrogenase, Fe-S protein subunit (I, H, O)				
C06A8.1		5,10-methylenetetrahydrofolate reductase (I, H, O)				
C01F1.3	Y	Putative NAD^+-dependent epimerases				

			Homologs[§]			
Sequence/gene name*	Causes protein aggregation[†]	Description (expression pattern)[‡]	*Hs*	*Dm*	*Cb*	*Sc*
C28H8.11		Tryptophan 2,3-dioxygenase (H, O)				
C03G5.1		Succinate dehydrogenase, flavoprotein subunit (I, H, O)				
H13N06.3/*gob-1*		Trehalose phosphate synthase				
Protein trafficking						
R06A4.4/*imb-2*		Nuclear transport receptor karyopherin-β2/transportin, importin β superfamily				
F38E11.5		Vesicle coat complex COPI, β' subunit				
F55C5.8		Signal recognition particle, subunit Srp68 (I, O)				
C37C3.3[¶]	Y	Protein involved in glucose derepression and prevacuolar endosome protein sorting (O)				
C02C6.1/*dyn-1*		Vacuolar sorting protein VPS1, dynamin, and related proteins (I, O)				
R160.1/*dpy-23*		Adaptor complexes medium subunit family				
Transcriptional regulation						
C01H6.5/*nhr-23*		Steroid hormone nuclear receptor (I, O)				

			Homologs[§]			
Sequence/gene name*	Causes protein aggregation[†]	Description (expression pattern)[‡]	*Hs*	*Dm*	*Cb*	*Sc*
F57B9.2/*ntl-1*	Y	Negative regulator of transcription				
C55A6.9		Putative RNA polymerase II regulator				
C01B10.5/*hil-7*		Histone H1.1 isoform				
K08E4.1/*spt-5*		RNA polymerase II transcription elongation factor DSIF/SUPT5H/SPT5 (I, O)				
ZC518.3/*ccr-4*		Glucose-repressible alcohol dehydrogenase transcriptional effector CCR4 and related proteins				
T22D1.10/*ruvb-2*		DNA helicase TIP49, TBP-interacting protein				
T28F12.2/*unc-62*		Transcription factor MEIS1 and related HOX domain proteins				
C27H6.2/*ruvb-1*		DNA helicase, TBP-interacting protein				
No assigned function						
T26C5.2[¶]		Unnamed protein. Contains a PAN domain that mediates protein–protein and protein–carbohydrate interactions				
ZC328.1		Unnamed protein				
Y110A7A.11		Predicted membrane protein				

			Homologs[§]			
Sequence/gene name*	Causes protein aggregation[†]	Description (expression pattern)[‡]	*Hs*	*Dm*	*Cb*	*Sc*
C32E12.3/*osr-1*[¶]		Unnamed protein (I, H)				
F23F1.4		Unnamed protein				
C50D2.1[¶]		Unnamed protein				
C38C6.3[¶]		Unnamed protein				
ZK1067.7/*pqn-95*[¶]		Uncharacterized protein (O)				
M88.6/*pan-1*[¶]		Leucine rich repeat protein				
C23G10.8		Unnamed protein (I, O)				
F20H11.6		Unnamed protein				
ZK1128.3		Unnamed protein				
Y111B2A.14/*pqn-80*		Ubinuclein, nuclear protein interacting with cellular and viral transcription factors				
T05D4.4[¶]		Unnamed protein				
W07B3.2/*gei-4*		Unnamed protein				

			Homologs[§]			
Sequence/gene name*	Causes protein aggregation[†]	Description (expression pattern)[‡]	*Hs*	*Dm*	*Cb*	*Sc*
F49C12.12[¶]	Y	Unnamed protein				
B0035.11		Uncharacterized conserved protein				
F52B11.3/*noah-1*[¶]	Y	Unnamed protein				
Y57G11C.31		Uncharacterized protein				
Y39B6A.1		Uncharacterized protein				
E01B7.1	Y	Uncharacterized protein				
F14H3.9		Uncharacterized protein				
Y39B6A.12		Uncharacterized protein				
F11C7.5[¶]		Unnamed protein				

*Sequence/gene name of gene targeted by RNAi.

[†]RNAi gene inactivations identified to cause protein aggregation by Nollen *et al*. (1).

[‡]Predicted functions were based mainly on KOG (eukaryotic orthologous groups) annotations as described in Wormbase. In some cases, function was inferred from the known function of homologs in other organisms. Expression patterns were determined based on information available in Wormbase; I, intestine (including foregut); H, hypodermis; O, other.

[§]Homologs were identified based on BLASTP analysis as implemented in Wormbase. *Hs*, *Homo sapiens*; *Dm*, *Drosophila melanogaster*; *Cb*, *Caenorhabditis briggsae*; *Sc*, *Sacchromyces cerevisea*. Green, strong homology (BLAST e < –50); yellow, weak homology (BLAST e > –50); white, no homologs.
[¶]Possible secreted protein. Prediction based on presence of signal peptide identified by using SignalP 3.0 (www.cbs.dtu.dk/services/SignalP).

1. Nollen, E. A., Garcia, S. M., van Haaften, G., Kim, S., Chavez, A., Morimoto, R. I. & Plasterk, R. H. (2004) *Proc. Natl. Acad. Sci USA* **101,** 6403–6408.

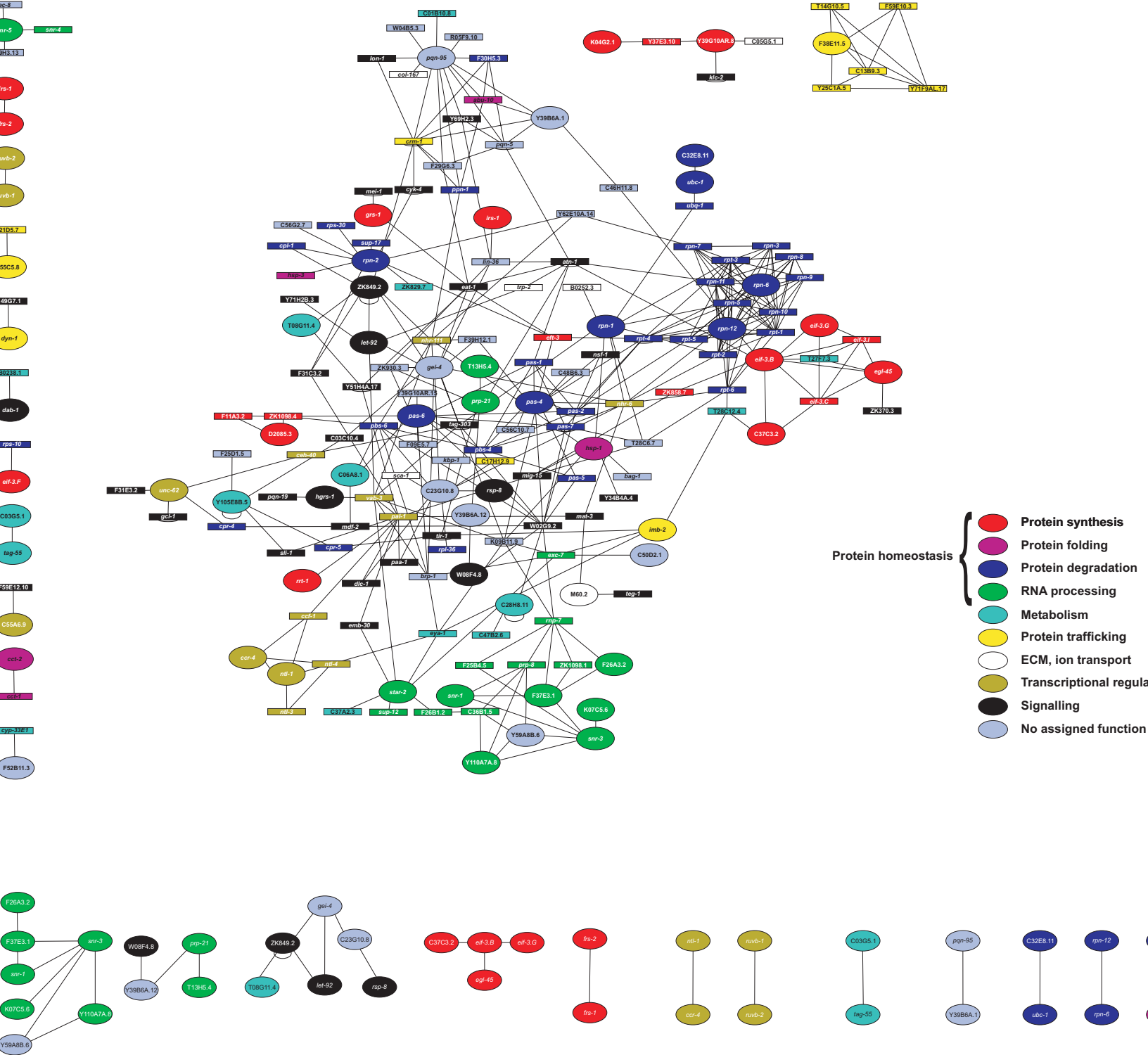
Protein homeostasis
Protein synthesis
Protein folding
Protein degradation
RNA processing
Metabolism
Protein trafficking
ECM, ion transport
Transcriptional regula
Signalling
No assigned function